JACS
JOURNAL OF THE AMERICAN CHEMICAL SOCIETY
Communication
pubs.acs.org/JACS

Monitoring Protein Capsid Assembly with a Conjugated Polymer Strain Sensor

Hande E. Cingil, Ingeborg M. Storm, Yelda Yorulmaz, Diane W. te Brake, Renko de Vries, Martien A. Cohen Stuart, and Joris Sprakel*

Physical Chemistry and Soft Matter, Wageningen University, Dreijenplein 6, 6703 HB Wageningen, The Netherlands

Supporting Information

ABSTRACT: Semiconducting polymers owe their optoelectronic properties to the delocalized electronic structure along their conjugated backbone. Their spectral features are therefore uniquely sensitive to the conformation of the polymer, where mechanical stretching of the chain leads to distinct vibronic shifts. Here we demonstrate how the optomechanical response of conjugated polyelectrolytes can be used to detect their encapsulation in a protein capsid. Coating of the sensor polymers by recombinant coat proteins induces their stretching due to steric hindrance between the proteins. The resulting mechanical planarizations lead to pronounced shifts in the vibronic spectra, from which the process of capsid formation can be directly quantified. These results show how the coupling between vibronic states and mechanical stresses inherent to conjugated polymers can be used to noninvasively measure strains at the nanoscale.

Conjugated polymers derive their unique optoelectronic properties from the characteristic delocalized electronic structure of the polymer backbone. For well-defined conjugated polymers, fluorescence spectra exhibit distinct vibronic bands, which are uniquely sensitive to the backbone conformation. These effects are often employed in the solid state to manipulate the band structure and optoelectronic properties of conjugated polymer films.[1−3] The transition from amorphous to semicrystalline order in the β-phase of polyfluorenes, is attributed to the planarization of the backbone that gives rise to distinct vibronic transitions of the molecule and a red-shifted emission.[4] Due to the mechanochromism which is widely reported also for polydiacetylene,[5−7] the conjugated polymer acts as a sensitive optical sensor for its own conformation.[8,9] This planarized β-phase of polyfluorenes is typically found and studied in the solid state.[10−13] In principle, this coupling between induced planarization and vibronic states may also occur when single molecules in solution are forced into an extended state. This holds the promise of using conjugated chains as molecular strain sensors to probe how supramolecular assembly triggers conformational changes or to probe strains in polymer networks at the single-molecule level.[14] One striking example of how supramolecular assembly can lead to mechanical stresses is the stiffening of polymers upon their grafting with side chains into a so-called bottlebrush structure.[15] This is for example encountered when DNA is encapsulated by viral coat proteins in the formation of rod-like viruses.[16] As the local concentration of coat proteins increases, lateral interactions between these individual building blocks increase the effective persistence length of the coassembled structure, upon which the DNA template stretches.[17] While binding processes can be studied directly using FRET,[18] the changes in the conformation of the macromolecules it encapsulates can only be deferred indirectly and are especially difficult to evaluate during early stages of capsid formation when stretching is modest.

In this paper we show how a water-soluble conjugated polyelectrolyte (CPE) can be used as a mechanosensor for the conformational changes it undergoes upon encapsulation in a protein capsid. The electrostatic complexation of a recombinant coat protein with an anionic polyfluorene derivative induces stretching of the template, resulting in distinct vibronic shifts in the fluorescence spectra of the polymer. Through calibration we demonstrate that this single molecule strain sensor shows high sensitivity even for low degrees of protein binding. Finally, we show how the same probe can be used to quantitatively determine capsid disintegration upon gradual weakening of the binding energy.

We start from a carboxylated polyfluorene derivative, poly[9,9′-bis(3′-propanoate)fluoren-2,7-yl] sodium salt (PF3), synthesized by Yamamoto coupling[19] (Figure 1A), which is soluble in water at pH > 7, with M_w = 16.7 kg/mol (PDI = 2.4); see Supporting Information for detailed information. Similar anionic conjugated polymers have been studied extensively for sensitive detection of multivalent charged species by superquenching.[20,21] While this approach offers excellent detection thresholds, measurement of quantum efficiency does not provide direct insight into the resulting chain conformation. Rather, we note that when these polymers are synthesized to be well-defined with few defects, their photoluminescence (PL) spectra exhibit distinct vibronic bands (Figure 1B), which are highly sensitive to the chain conformation.

To induce stretching of the PF3 we use a neutral-cationic polypeptide diblock C_4B^{K12} (Figure 1A), which is inspired by natural protein capsid formers and biosynthetically produced in a recombinant *Pichia pastoris* host. It is a minimal design for a coat protein composed of two blocks: the weakly zwitterionic and hydrophilic, stabilizing coil block (C_4) that consists of 400 amino acids, maintains a random coil structure with a radius of gyration of 7 nm, and ensures colloidal stability and the cationic binding block (B^{K12}) consisting of 12 lysine residues. C_4B^{K12} has previously shown to be capable of physically attaching to single

Received: June 8, 2015
Published: July 31, 2015

DOI: 10.1021/jacs.5b05914
J. Am. Chem. Soc. 2015, 137, 9800−9803

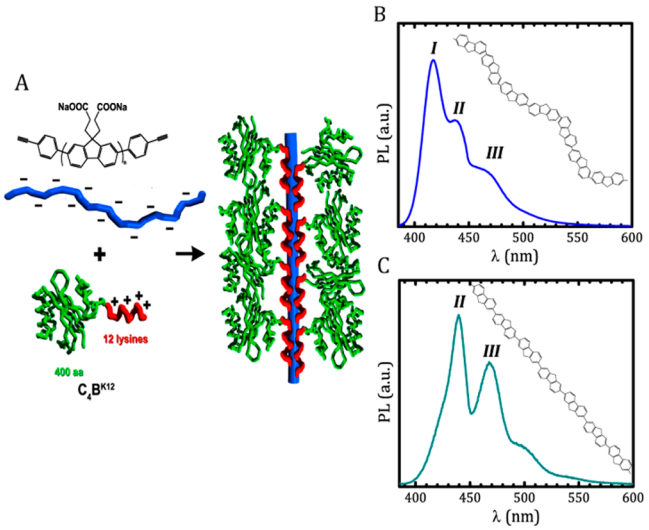

Figure 1. Schematic illustration of the structure of the polyfluorene-based sensor polyelectrolyte PF3 and the coat protein C_4B^{K12} (A). PL spectra of bare and flexible PF3 (B) and of stretched PF3 after coating with C_4B^{K12} (C).

DNA molecules forming a stable coat[22] while inducing an effective stiffening of the chain.[15,17,23] The mixing ratio between PF3 and protein is expressed as the molar ratio of cationic charges to the total number of charges $f+ = [+]/([-] + [+])$. For all experiments we work under dilute conditions of the PF3 (c = 0.03 mM) to avoid intramolecular radiative transfer, unless stated otherwise, in the absence of added salt, at pH = 8.5, at 22 °C. The bare PF3 in its native, dissolved state exhibits significant chain flexibility that allows out-of-plane rotations of the backbone which reduce its effective conjugation length. In this scenario we observe three distinct vibronic bands in its fluorescence spectra (Figure 1B), with a main band I at 418 nm and two weaker bands, II and III, at 436 and 465 nm, respectively. These bands correspond to the 0−0, 0−1, and 0−2 vibronic transition within the Franck−Condon description. In its coated state, after complexation with the coat protein, a bathochromic shift of ∼3 nm occurs. More distinctly, we observe distinct changes in the vibronic peaks, where band I is significantly quenched, except for a small shoulder at ∼415 ver, a shoulder corresponding to the 0−3 transition is discernible around 505 nm. Upon titrating C_4B^{K12} to PF3 in small increments, we observe a distinct broadening of the absorption spectra toward lower energies (Figure 2A). More pronouncedly, the binding that ensues triggers a gradual transition from the PL spectrum of the bare PF3 to the fully coated state (Figure 2B). The intensity from the lowest vibronic transition decays smoothly and simultaneously; bands II and III grow in intensity with increasing $f+$ (inset Figure 2B). This characteristic change in the vibronic states is also observed when amorphous polyfluorene transforms into a planarized state known as the β-phase.[4,9,10,24] In this ordered state, observed in the solid state of well-defined alkyl-functionalized polyfluorenes, intramolecular chain interactions force the polymers to stretch, reducing rotational degrees of freedom and thereby increasing the effective conjugation length. This raises the intriguing possibility that the vibronic shifts we observe upon protein binding are the direct result of the stretching and planarization of the conjugated polyelectrolyte due to electrostatic complexation with the coat protein. Interestingly, the previously reported effect of superquenching,[17,18] which detects binding rather than chain stretching, is also observed here (Supp. Figure 1), thus, suggesting the possibility that binding and stretching can be detected independently with the same molecular sensor. To confirm that the observed vibronic shifts are due to stretching of the chain and not due to the charge compensation itself, we repeat the experiment above with a polylysine homopolymer. This polypeptide binds to the anionic polyfluorene but lacks the stabilizing block which is responsible for the lateral interactions between grafts that lead to an increase in main-chain persistence length. Upon mixing the anionic polyfluorene with polylysine a liquid-like coacervate forms, in which chains adopt a largely screened coil-like conformation.[25] While we observe strong quenching of the PL (inset Figure 2C), reported previously to result from binding,[17,18] the characteristic vibronic shifts, which we attribute to stretching, remain absent (Figure 2C). This indeed suggests that vibronic spectroscopy can be used to sensitively monitor conformational changes in single conjugated chains in solution. While the sensor polymer exhibits significant polydispersity, the vibronic spectra are mostly sensitive to local effects at the scale of the conjugation length; since the average local protein density is independent of PF3 length, polydispersity effects are expected not to be of major significance.

We further verify this by determining the structure of the complexes by means of synchrotron small-angle X-ray scattering.

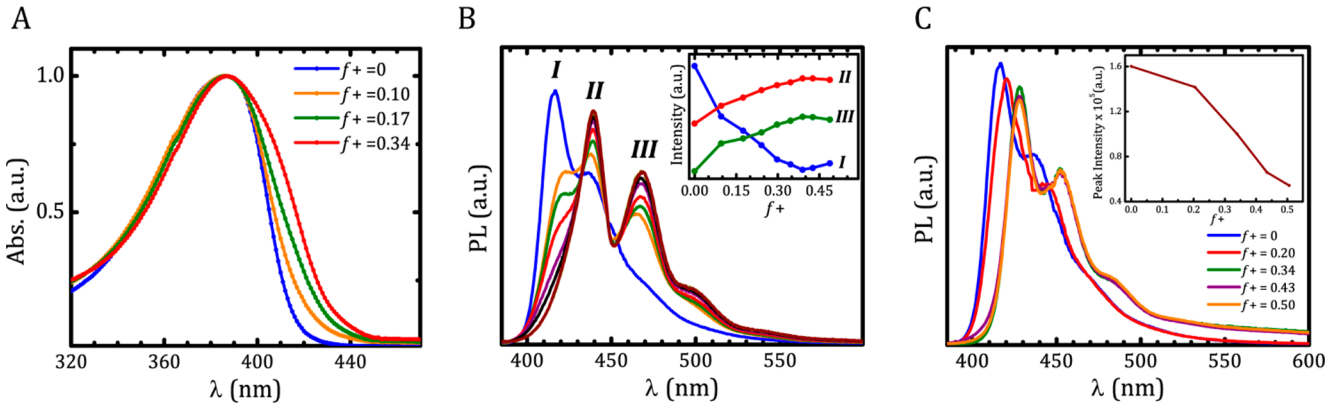

Figure 2. Absorption spectra for PF3 at different mixing ratios $f+$ with the diblock protein C_4B^{K12} (A); corresponding normalized PL spectra with inset showing the intensity change of vibronic bands I, II, and III (B); Normalized PL spectra of bare PF3 compared to its complex formed with poly(lysine) homopolymer at mixing ratio $f+$ = 0.5 with inset showing the corresponding maximum peak intensity as a function of mixing ratio, illustrating the superquenching effect (C).

DOI: 10.1021/jacs.5b05914
J. Am. Chem. Soc. 2015, 137, 9800−9803

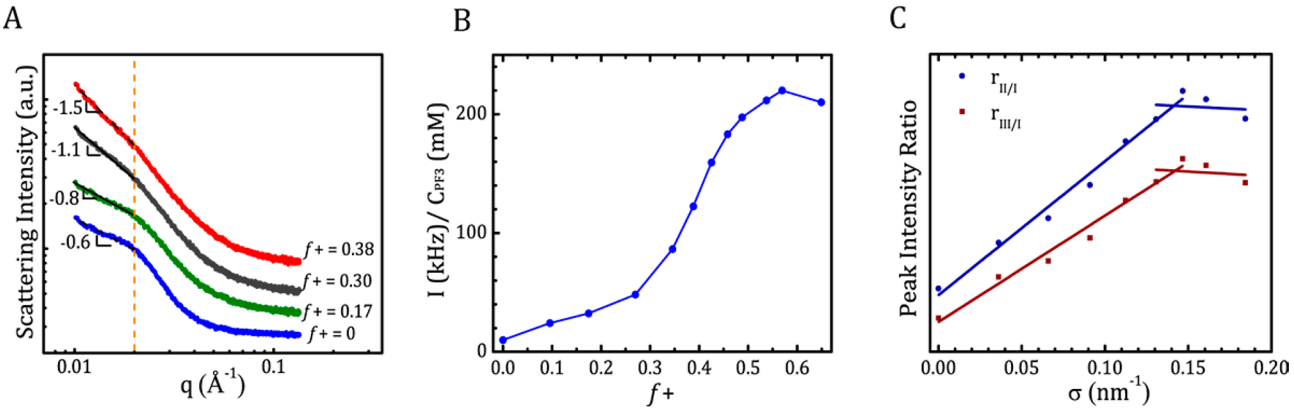

Figure 3. Small angle X-ray scattering intensity as a function of wave vector q. The dotted line indicates the limits of the Guinier regime where $I(q) \propto q^{-\alpha}$, with the slope α indicated for each mixing ratio $f+ = 0$ ($\sigma = 0$), $f+ = 0.17$ ($\sigma = 0.066$), $f+ = 0.30$ ($\sigma = 0.112$), $f+ = 0.38$ ($\sigma = 0.146$) (A). Light scattering intensity, corrected for dilution, as a function of mixing ratio indicating saturation of binding at charge compensation $f+ \approx 0.5$ (B). Sensor calibration given as the ratio of peak intensities $r_{II/I}$ and $r_{III/I}$ as a function of the estimated grafting density σ (C).

For dilute solutions of scatterers with typical dimension R, the Guinier regime, found at small scattering vectors $qR < 1$, exhibits a power law decay $I(q) \propto q^{-\alpha}$. The exponent α is related to the structure of the scattering objects; $\alpha = 0$ indicates an isotropic coil-like conformation while $\alpha > 0$ signals a stretched and anisotropic conformation.[8,26] The bare PF3 exhibits a slope of $\alpha \approx 0.6$, indicating a semiflexible chain intermediate between rod and coil, which can be explained by the relatively high Kuhn length of 7−9 nm,[27] compared to its contour length of $l_c \approx 45$ nm (Figure 3A). As protein binds to the polymer, we indeed observe stiffening and stretching of the PF3 chains as the exponent increases significantly. The fact that α becomes larger than unity indicates the formation of a ribbon-like structure when the CP, together with its physically grafted protein side chains, extends and planarizes. This has also been observed for alkyl-functionalized polyfluorenes during β-phase formation.[28] For flexible polymers, such electrostatic interactions would lead to the formation of spherical objects, driven by coacervate surface tension; however, the intrinsic stiffness of the PF3 causes anisotropic objects.

To calibrate the strain sensor, we use light scattering to confirm that binding saturates at full charge compensation, seen as a plateau in concentration-corrected scattering intensity at $f+ \approx 0.5$ (Figure 3B). From this, assuming tight binding, we estimate that, at $f+ \approx 0.5$, on average 8.5 proteins with 12 cationic groups bind to each PF3 chain which has ∼100 negative charges. This allows us to construct a calibration curve of the ratio of vibronic band intensities, $r_{II/I}$ and $r_{III/I}$, as a function of grafting density σ, which is the number of side grafts per unit length of the backbone (Figure 3C). We find a linear relation between $r_{II/I}$ *and* $r_{III/I}$, and grafting density for $\sigma < 0.14$ nm^{-1}. In this regime, we can thus accurately detect and quantify the protein binding on the PF3 backbone from the stretching it induces. Interestingly, at grafting densities $\sigma > 0.14$ nm^{-1}, below the maximum grafting density $\sigma_{max} = 0.19$ nm^{-1} at full charge compensation, the vibronic signal saturates (Figure 3C). This saturation effect can be explained by considering how binding of the coat protein induces an effective stiffening of the PF3. The polymeric sensor is composed of $N_s \approx 50$ statistical segments of dimension $a_s = 0.9$ nm, with a contour length $l_c = N_s a_s \approx 45$ nm. This backbone is decorated with pendant protein grafts, consisting of the C_4 block composed of $N_g = 400$ amino acids with dimension $a_g \approx 0.3$ nm. The grafting density σ is related to the number of bound protein grafts n_g, as $\sigma = n_g/N_s a_s$. The presence of the grafted chains provides additional resistance to bending of the backbone, leading to an effective increase in persistence length $l_p \approx N_g^2 \nu a_g^3 \sigma^2 = N_g^2 \nu a_g^3 \sigma^2 n_g^2 / N_s^2 a_s^2$, where ν is the dimensionless second virial coefficient, which is 0.5 in a good solvent.[12] At saturation, $\sigma = 0.14$ nm^{-1}, the effective persistence length of the grafted PF3 $l_p \approx 42$ nm becomes almost equal to the contour length of the sensor polymer. Saturation of the vibronic shift thus occurs when $l_p \approx l_c$; binding of additional proteins beyond this point no longer induces further stretching, which results in a plateau in the ratio of vibronic peak intensities. This indicates that the sensitivity and saturation threshold of the conformation sensors can be tailored in the sensor design by means of, for example, its degree of polymerization N_g.

The binding between C_4B^{K12} and PF3 is the result of electrostatic interactions. Consequently, the binding strength should depend sensitively on the ionic strength of the aqueous solution due to screening of the Coulombic interactions between the oppositely charged polyelectrolytes. The conformational changes upon binding of the protein should be reversible upon addition of salt. We start with complexes formed at $f+ = 0.2$, in the absence of added salt, and gradually titrate the solution with a 5 M NaCl solution. As the ionic strength increases, resulting in weakening of the electrostatic bonds, we observe a reversal of the vibronic shifts reported above; the intensity of the first vibronic peak I increases, while bands II and III gradually quench (Figure 4A). This trend can be followed in the inset of Figure 4A which shows the change in the vibronic signature of PF3 with increasing salt concentration. This confirms that, upon addition of salt, binding is gradually suppressed; thereby, PF3 returns to its semiflexible, uncoated state. Using the calibration curve in Figure 3C, we also directly quantify the protein binding density along the polymer backbone as a function of ionic strength. With increasing salt concentration, the density of bound proteins decreases linearly (Figure 4C); the data suggest that the electrostatic complexes disintegrate completely at [NaCl] ≈ 1.2 M, which is consistent with the observed dissolution of complexes between oppositely charged synthetic polymers.[29]

These results highlight how vibronic spectroscopy on simple π-conjugated polyelectrolytes can be used to directly and noninvasively detect their conformational state in solution. The coupling of vibrational and electronic states in anionic polyfluorenes, resulting in distinct vibronic fingerprints, allows sensitive and quantitative detection of how supramolecular interactions lead to changes in the configuration of a single

DOI: 10.1021/jacs.5b05914
J. Am. Chem. Soc. 2015, 137, 9800−9803

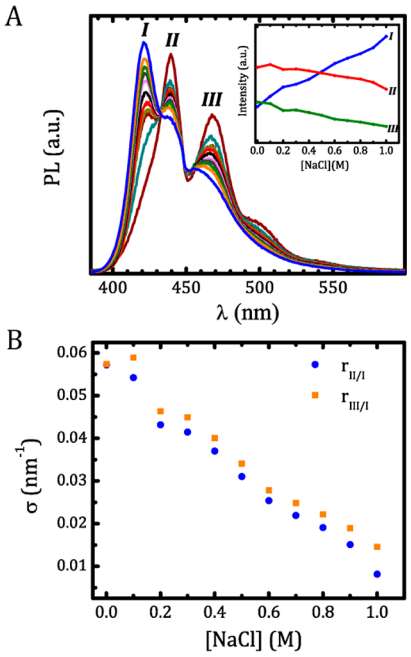

Figure 4. Reversibility assay where a preassembled electrostatic complex of capsid forming protein C_4B^{K12} and PF3 is titrated with indifferent electrolyte: the normalized PL spectra with the inset showing the corresponding change in normalized vibronic band intensities (A); grafting density as a function of ionic strength is determined from the sensor calibration given above (B).

polymer chain. Combined with their superquenching ability, this offers a complete tool for studying the kinetics of binding and resulting shape transformations in the supramolecular assemblies. Moreover, we envision that the intimate connection between the stretching of single chains with spectral response, as demonstrated here, opens new possibilities to measure local strains in the mechanical testing of bulk materials, such as gels or elastomers, to give molecular insight into the mechanisms of deformation and failure.

■ ASSOCIATED CONTENT

Supporting Information

The Supporting Information is available free of charge on the ACS Publications website at DOI: 10.1021/jacs.5b05914.

Details on synthesis; characterization and experimental conditions with extra figures; and NMR, MALDI-TOF, and SDS-PAGE results (PDF)

■ AUTHOR INFORMATION

Corresponding Author

*joris.sprakel@wur.nl

Notes

The authors declare no competing financial interest.

■ ACKNOWLEDGMENTS

This work was financially supported by a European Research Council Advanced Grant (ERC-267254). Authors would like to thank Dr. Eric M. M. Tan for the schematic illustrations.

■ REFERENCES

(1) Kuehne, A. J. C.; Kaiser, M.; Mackintosh, A. R.; Wallikewitz, B. H.; Hertel, D.; Pethrick, R. A.; Meerholz, K. *Adv. Funct. Mater.* **2011**, *21*, 2564.
(2) Rothe, C.; Galbrecht, F.; Scherf, U.; Monkman, A. *Adv. Mater.* **2006**, *18*, 2137.
(3) Khan, A. L. T.; Sreearunothai, P.; Herz, L. M.; Banach, M. J.; Kohler, A. *Phys. Rev. B* **2004**, *69*, 085201.
(4) Cadby, A. J.; Lane, P. A.; Mellor, H.; Martin, S. J.; Grell, M.; Giebeler, C.; Bradley, D. D. C.; Wohlgenannt, M.; An, C.; Vardeny, Z. V. *Phys. Rev. B: Condens. Matter Mater. Phys.* **2000**, *62*, 15604.
(5) Nallicheri, R. A.; Rubner, M. F. *Macromolecules* **1991**, *24*, 517.
(6) Carpick, R. W.; Sasaki, D. Y.; Burns, A. R. *Langmuir* **2000**, *16*, 1270.
(7) Park, D. H.; Hong, J.; Park, I. S.; Lee, C. W.; Kim, J. M. *Adv. Funct. Mater.* **2014**, *24*, 5186.
(8) Da Como, E.; Becker, K.; Feldmann, J.; Lupton, J. M. *Nano Lett.* **2007**, *7*, 2993.
(9) Becker, K.; Lupton, J. M. *J. Am. Chem. Soc.* **2005**, *127*, 7306.
(10) Dias, F. B.; Morgado, J.; Maçanita, A. L.; Da Costa, F. P.; Burrows, H. D.; Monkman, A. P. *Macromolecules* **2006**, *39*, 5854.
(11) Knaapila, M.; Torkkeli, M.; Monkman, A. P. *Macromolecules* **2007**, *40*, 3610.
(12) Rosencrantz, R. R.; Rahimi, K.; Kuehne, A. J. C. *J. Phys. Chem. B* **2014**, *118*, 6324.
(13) Evans, R. C.; Marr, P. C. *Chem. Commun.* **2012**, *48*, 3742.
(14) Ducrot, E.; Chen, Y. L.; Bulters, M.; Sijbesma, R. P.; Creton, C. *Science* **2014**, *344*, 186.
(15) Feuz, L.; Leermakers, F. A. M.; Textor, M.; Borisov, O. *Macromolecules* **2005**, *38*, 8891.
(16) Knobler, C. M.; Gelbart, W. M. *Annu. Rev. Phys. Chem.* **2009**, *60*, 367.
(17) Zhang, C.; Hernandez-Garcia, A.; Jiang, K.; Gong, Z. Y.; Guttula, D.; Ng, S. Y.; Malar, P. P.; van Kan, J. A.; Dai, L.; Doyle, P. S.; de Vries, R.; van der Maarel, J. R. C. *Nucleic Acids Res.* **2013**, *41*, DOI: 10.1093/nar/gkt783.
(18) Rao, V. B.; Black, L. W. *Virol. J.* **2010**, *7*, DOI: 10.1186/1743-422X-7-356.
(19) Cho, S. Y.; Grimsdale, A. C.; Jones, D. J.; Watkins, S. E.; Holmes, A. B. *J. Am. Chem. Soc.* **2007**, *129*, 11910.
(20) Kumaraswamy, S.; Bergstedt, T.; Shi, X. B.; Rininsland, F.; Kushon, S.; Xia, W. S.; Ley, K.; Achyuthan, K.; McBranch, D.; Whitten, D. *Proc. Natl. Acad. Sci. U. S. A.* **2004**, *101*, 7511.
(21) Fan, C. H.; Wang, S.; Hong, J. W.; Bazan, G. C.; Plaxco, K. W.; Heeger, A. J. *Proc. Natl. Acad. Sci. U. S. A.* **2003**, *100*, 6297.
(22) Hernandez-Garcia, A.; Werten, M. W. T.; Stuart, M. C.; de Wolf, F. A.; de Vries, R. *Small* **2012**, *8*, 3491.
(23) Storm, I. M.; Kornreich, M.; Hernandez-Garcia, A.; Voets, I. K.; Beck, R.; Stuart, M. A. C.; Leermakers, F. A. M.; de Vries, R. *J. Phys. Chem. B* **2015**, *119*, 4084.
(24) Grell, M.; Bradley, D. D. C.; Ungar, G.; Hill, J.; Whitehead, K. S. *Macromolecules* **1999**, *32*, 5810.
(25) Spruijt, E.; Leermakers, F. A. M.; Fokkink, R.; Schweins, R.; van Well, A. A.; Stuart, M. A. C.; van der Gucht, J. *Macromolecules* **2013**, *46*, 4596.
(26) Knaapila, M.; Bright, D. W.; Stepanyan, R.; Torkkeli, M.; Almásy, L.; Schweins, R.; Vainio, U.; Preis, E.; Galbrecht, F.; Scherf, U.; Monkman, A. P. *Phys. Rev. E: Stat., Nonlinear, Soft Matter Phys.* **2011**, *83*, 051803.
(27) Fytas, G.; Nothofer, H. G.; Scherf, U.; Vlassopoulos, D.; Meier, G. *Macromolecules* **2002**, *35*, 481.
(28) Knaapila, M.; Dias, F. B.; Garamus, V. M.; Almásy, L.; Torkkeli, M.; Leppänen, K.; Galbrecht, F.; Preis, E.; Burrows, H. D.; Scherf, U.; Monkman, A. P. *Macromolecules* **2007**, *40*, 9398.
(29) Voets, I. K.; de Keizer, A.; Stuart, M. A. C. *Adv. Colloid Interface Sci.* **2009**, *147-148*, 300.

DOI: 10.1021/jacs.5b05914
J. Am. Chem. Soc. 2015, 137, 9800−9803